

RSC Advances



This is an *Accepted Manuscript*, which has been through the Royal Society of Chemistry peer review process and has been accepted for publication.

Accepted Manuscripts are published online shortly after acceptance, before technical editing, formatting and proof reading. Using this free service, authors can make their results available to the community, in citable form, before we publish the edited article. This *Accepted Manuscript* will be replaced by the edited, formatted and paginated article as soon as this is available.

You can find more information about *Accepted Manuscripts* in the [Information for Authors](#).

Please note that technical editing may introduce minor changes to the text and/or graphics, which may alter content. The journal's standard [Terms & Conditions](#) and the [Ethical guidelines](#) still apply. In no event shall the Royal Society of Chemistry be held responsible for any errors or omissions in this *Accepted Manuscript* or any consequences arising from the use of any information it contains.

Cite this: DOI: 10.1039/c0xx00000x

www.rsc.org/xxxxxx

ARTICLE TYPE

Electrochemically activated graphite electrode with excellent kinetics of electrode processes of V(II)/V(III) and V(IV)/V(V) couples in a vanadium redox flow battery

Huijun Liu^{*a}, Lingxu Yang^b, Qian Xu^b and Chuanwei Yan^a

Received (in XXX, XXX) Xth XXXXXXXXX 20XX, Accepted Xth XXXXXXXXX 20XX

DOI: 10.1039/b000000x

The electrochemically activated graphite electrode (EAGE) is obtained by a simple and moderate method of anodic potentiostatic polarization. The composition, microstructure, and electrochemical properties of EAGE are characterized by high resolution X-ray photoelectron spectroscopy, high resolution transmission electron microscopy, cyclic voltammetry and electrochemical impedance spectroscopy. The results show that the electrochemical activity and the reversibility for electrode processes of V(II)/V(III) and V(IV)/V(V) couples on EAGE are significantly improved due to the introduced C=O and COOH groups. The rate constant of charge transfer for the anodic oxidation of V(IV) on EAGE is evaluated as $8.17 \times 10^{-4} \text{ cm} \cdot \text{s}^{-1}$, which is about 20 times larger than that on the pristine graphite electrode of $4.09 \times 10^{-5} \text{ cm} \cdot \text{s}^{-1}$.

1. Introduction

The vanadium redox flow battery (VRFB), as a promising technology for large-scale energy storage, has been attracted more and more attention due to its advantages such as long cycle life, fast response time, deep-discharge capability, and low pollution emitting.¹⁻⁴ Carbon based materials have been reported to be the major electrode materials in VRFB, such as graphite felt,⁵ carbon paper,⁶ carbon coating,^{7,8} carbon fiber,⁹ and so on. However, these carbon based electrode materials have been proved to own poor electrochemical activity and kinetic reversibility. In fact, considerable efforts have been devoted to enhance the electrochemical activity of carbon based materials by increasing functional groups, which can catalyze the electrochemical reaction of vanadium ion redox couples.¹⁰⁻¹⁶ The graphite electrode is electrochemically activated by electrochemical method in this investigation and the objective is to investigate the effect of electrochemical activation on kinetics of electrode processes of V(II)/V(III) and V(IV)/V(V) couples by cyclic voltammetry and electrochemical impedance spectroscopy. It should be possible to gain a simple and moderate method to improve the electrochemical activity of the carbon based electrode.

2. Experimental

2.1 Sample preparation

The electrochemically activated graphite electrode (EAGE) was

obtained by anodic potentiostatic polarization of the graphite electrode, which was described in the literature,¹⁷ at 1.8 V vs. saturated calomel electrode (SCE) for 2 h in 2 mol dm⁻³ H₂SO₄ solution at the bath temperature of 20 °C.

2.2 Characterization of graphite electrode

The flake of the graphite was peeled off from the surface of the electrode before and after electrochemical activation for further characterization. The high resolution transmission electron microscopy (HRTEM) was obtained by using a JEOL-2100F at an accelerating voltage of 200 kV. High resolution X-ray photoelectron spectroscopy (HRXPS) with a resolution of 0.1 eV was obtained with ESCALAB250 XPS (Thermo VG, USA) at 5.5×10^{-8} mbar. Al-K α (1486.6 eV) was used as X-ray source at 15 kV of anodic voltage. Spectra were analyzed using Spectrum software (XPSPEAK41).

2.3 Electrochemical measurements

The cyclic voltammetry (CV) and electrochemical impedance spectroscopy (EIS, frequency range from 10⁻² to 10⁵ Hz, amplitude of 5 mV) were carried out on PARSTAT 2273-potentiostat/galvanostat/FRA by a conventional three-electrode cell. The reference electrode was a SCE, the counter electrode was a graphite plate with the dimension of 50 mm×60 mm×2 mm, and the working electrode was the pristine graphite electrode and EAGE as described in section 2.1. The electrolytes used were 2 mol dm⁻³ VOSO₄ + 2 mol dm⁻³ H₂SO₄ and 2 mol dm⁻³ V(III) + 2 mol dm⁻³ H₂SO₄ for the positive and negative, respectively. All chemicals were of analytical grade, and de-ionized water was

used for all experimental solutions. In addition, all the potentials are quoted with reference to SCE (0.242 V vs. normal hydrogen electrode) unless otherwise stated.

3. Results and discussion

3.1 Composition and microstructure characterization

The representative HRXPS C1s spectra of the pristine graphite electrode and EAGE are fitted and shown in Fig. 1. From Fig. 1a, the position of the main C1s peak at 284.5-284.7 eV implies that the carbon is present in graphite form.¹⁸ The C1s peak at 285.0-285.5 eV is attributed to the carbon in C-OH and C-O-C groups and the $\pi-\pi^*$ transition is detected at 290 eV.^{19,20} By comparison with Fig. 1a, another two new peaks of the carbon in C=O and COOH groups, respectively, at 286.3 and 288.4 eV are introduced on EAGE as shown in Fig. 1b.²¹⁻²³ In addition, the O content and the O/C ratio on EAGE reach to 17.01% and 0.205, compared to 9.0% and 0.10 of the pristine graphite electrode, respectively. These results further indicate that the C=O and COOH groups are introduced on the surface of EAGE. The functional groups of C=O and COOH introduced on EAGE may improve the hydrophilicity and affect the property of electronic structure of the graphite electrode because both of the groups are hydrophilic which can improve the properties of the electrode especially the ion adsorption ability. Therefore, they can directly affect the reaction kinetics and mechanism by providing specific reaction or adsorption sites for vanadium redox couples.²⁴ In other words, they may act as the reactive sites which are supposed to catalyze the redox processes of vanadium ions.

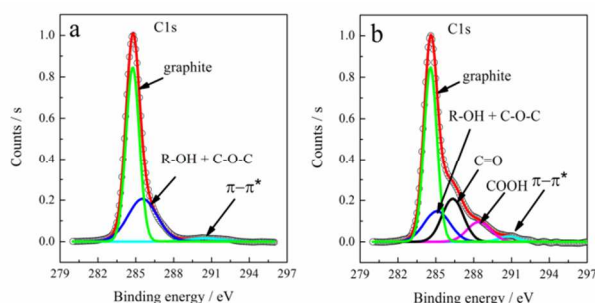


Fig. 1. C1s HRXPS spectra of the pristine graphite electrode (a) and EAGE (b)

Fig. 2 shows HRTEM images of the pristine graphite and EAGE. It is obvious that the pristine graphite is flaky with flat and smooth surface as shown in Fig. 2a. The lamellar structure of the graphite flakes can be observed at the edge of the graphite flakes from the detail view as shown in Fig. 2b. However, after electrochemical activation, the flat and smooth surface is damaged and became rough as shown in Fig. 2c. In addition, lots of edge plane sites and defect sites at the edge of graphite flake, comparison with the pristine graphite as shown in Fig. 2b, can be observed from the detail view as shown in Fig. 2d. These increased edge plane and defects site are supposed to provide more active adsorb sites or reactive places for the vanadium ions reactions. By comparison with Fig. 2b and combine with XPS analysis shown in Fig. 1, These edge plane and defect sites may be the C=O and COOH groups introduced during electrochemical activation because the carbon atoms at the edge of graphite flake

are more active and easier to be oxidized.²⁵

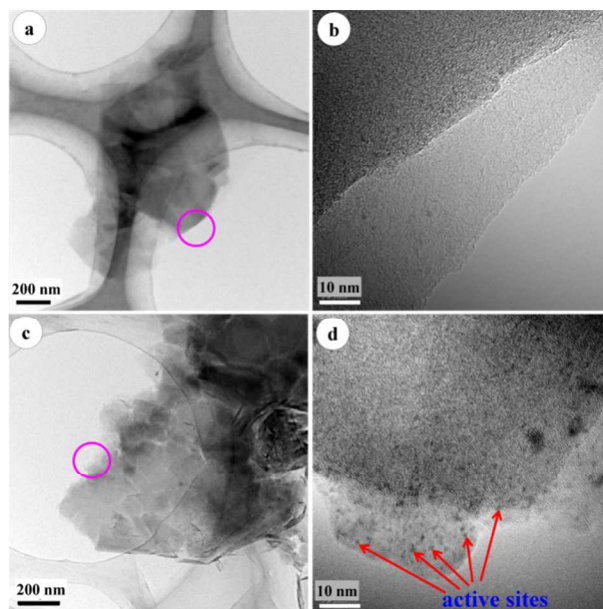


Fig. 2. HRTEM images and its detail view of the pristine graphite electrode (a and b) and EAGE (c and d)

3.2 Cyclic voltammetry and electrochemical impedance spectroscopy behavior

The cyclic voltammograms of the pristine graphite electrode and EAGE in 2 mol·dm⁻³ H₂SO₄+2 mol·dm⁻³ VOSO₄ solution at the scan rate of 5 mV·s⁻¹ are shown in Fig. 3. It is obvious that three pairs of oxidation and reduction peaks of O₁/R₁, O₂/R₂, and O₃/R₃ appear on EAGE, which are corresponding to the oxidation and reduction peaks of V(II)/V(III), V(III)/ V(IV), and V(IV)/V(V) couples, respectively. However, only one pair of oxidation and reduction peaks of V(IV)/V(V) couple is observed on the pristine graphite electrode as shown in Fig. 3. In addition, all of the electrochemical processes for the vanadium ion redox couples are apparently quasi-reversible on EAGE, but the ratios of the anodic peak and cathodic peak current for V(II)/V(III), V(III)/ V(IV), and V(IV)/V(V) couples are mostly close to 1:1. Furthermore, by comparison with the pristine graphite electrode, the peak current density of V(IV)/V(V) couple on EAGE is significantly enhanced. The most important thing is that the peaks at the 0.35 V and 0.03 V are observed on EAGE, which are supposed to be the redox reactions of the V(III)/ V(IV) and infrequently observed and seldom discussed in previous literatures.²⁶ All of these reveal that V(II)/V(III), V(III)/ V(IV), and V(IV)/V(V) couples on EAGE display better electrochemical activity and reversibility than that on the pristine graphite electrode, especially for V(II)/V(III), and V(III)/ V(IV) couples. According to section 3.1, This may be due to the electrochemical oxidation and reduction of V(II)/V(III), V(III)/V(IV), and V(IV)/V(V) couples can be catalyzed by the functional groups of COOH and C=O introduced on EAGE because of the carbon-oxygen functional groups involving in the mechanism of electrochemical processes for the vanadium ion redox couples.^{15, 27} Meanwhile, Some studies have indicated that the surface defects and edge-plane sites can facilitate the electron transfer and make the vanadium ions reaction much easier than that on the basal

plane.²⁸⁻³⁰ Therefore, the catalytic mechanism is presumed as described following. Because of the oxygen functional groups of COOH and C=O introduced on EAGE, more reactive vanadium ions can be adsorbed onto the EAGE surface, the electron transfer and oxygen transfer processes can also be catalyzed and become more faster on the EAGE than on the pristine graphite electrode. Therefore, the EAGE becomes more active towards the vanadium ions, which makes the reaction currents density larger than those of the pristine graphite electrode.

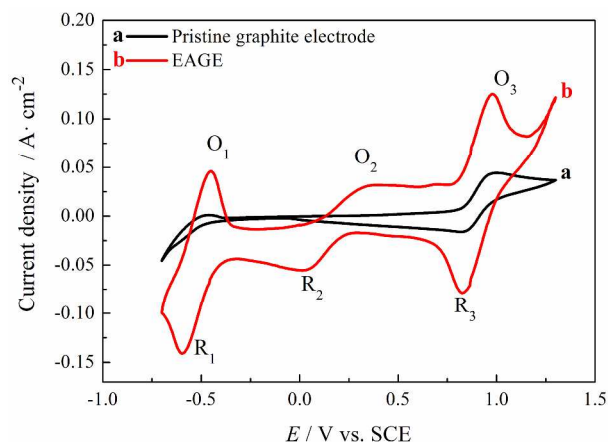


Fig. 3. The cyclic voltammograms of the pristine graphite electrode (a) and EAGE (b) in $2 \text{ mol}\cdot\text{dm}^{-3} \text{ H}_2\text{SO}_4+2 \text{ mol}\cdot\text{dm}^{-3} \text{ VOSO}_4$ solution at the scan rate of $5 \text{ mV}\cdot\text{s}^{-1}$

The cyclic voltammograms of the pristine graphite electrode and EAGE in $2 \text{ mol}\cdot\text{dm}^{-3} \text{ H}_2\text{SO}_4+2 \text{ mol}\cdot\text{dm}^{-3} \text{ VOSO}_4$ solution with different scan rates are shown in Fig. 4. It reveals that, for a given scan rate, both the anodic peak and the cathodic peak current density (i_p) of V(IV)/V(V) couple are enhanced on EAGE, e.g., the peak current density for the anodic oxidation of V(IV) and cathodic reduction of V(V) increases from 0.150 and $0.100 \text{ A}\cdot\text{cm}^{-2}$ to 0.346 and $0.287 \text{ A}\cdot\text{cm}^{-2}$, respectively, at the scan rate of $20 \text{ mV}\cdot\text{s}^{-1}$. In addition, the peak potential separation (ΔE_p) decreases from 103 to 61 mV at the scan rate of $10 \text{ mV}\cdot\text{s}^{-1}$. These suggest that the reaction rate of anodic and cathodic processes of V(IV)/V(V) couple on EAGE are much higher than that on the pristine graphite electrode.

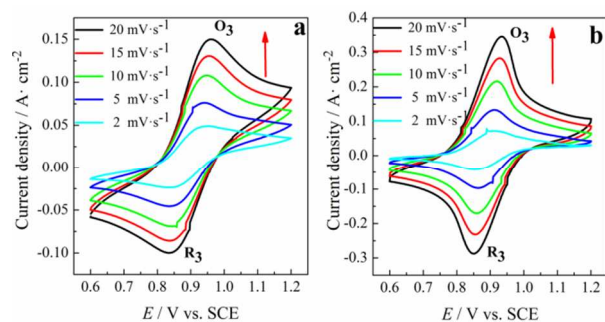


Fig. 4. The cyclic voltammograms of the pristine graphite electrode (a) and EAGE (b) in $2 \text{ mol}\cdot\text{dm}^{-3} \text{ H}_2\text{SO}_4+2 \text{ mol}\cdot\text{dm}^{-3} \text{ VOSO}_4$ solution with different scan rates.

As we known, for an irreversible electrode process, the peak current of the cyclic voltammogram can be described as following Eq. (1), thus the standard rate constant, k_0 , can be

evaluated by cyclic voltammograms.³¹

$$i_p = 0.227nFAC_b k_0 \exp[-\alpha nF(E_p - E_0)/RT] \quad (1)$$

where A is area of the electrode (cm^2), C_b is bulk concentration of V(IV) ion ($\text{mol}\cdot\text{dm}^{-3}$), α is charge transfer coefficient, E_0 is the equilibrium potential, Other symbols in the equation have their usual electrochemical significance. According to the typical examples of cyclic voltammograms shown in Fig. 4, the relationship between $\ln i_p$ and $(E_p - E_0)$ for the oxidation of V(IV) on the pristine graphite electrode and EAGE in $2 \text{ mol}\cdot\text{dm}^{-3} \text{ H}_2\text{SO}_4+2 \text{ mol}\cdot\text{dm}^{-3} \text{ VOSO}_4$ solution can be obtained and shown in supporting information Fig. S1. The plots have a slope of $-\alpha nF/RT$ and an intercept proportional to the standard rate constant, k_0 . Therefore, k_0 can be evaluated by extending the linear region of the plots to $E_p - E_0 = 0$. The rate constant of charge transfer for the anodic oxidation of V(IV), k_0 , on EAGE is evaluated as $8.17 \times 10^{-4} \text{ cm}\cdot\text{s}^{-1}$, which is about 20 times larger than that on the pristine graphite electrode of $4.09 \times 10^{-5} \text{ cm}\cdot\text{s}^{-1}$ (see supporting information Fig. S1a and S1b). According to Sun and Skyllas-Kazacos's reports that the oxygen functional groups on the carbon felts can facilitate the reactions of the V(IV)/V(V) redox reactions because the oxidation and reduction processes of V(IV)/V(V) involving the transfer of an oxygen atom.^{13, 32}

Therefore, we can conclude that the kinetics of electrode process of V(IV)/V(V) couple are significantly improved by functional groups of COOH and C=O introduced on graphite electrode by electrochemical activation.

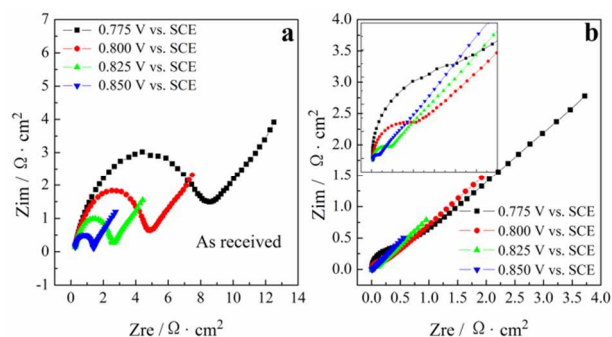


Fig. 5. Nyquist plots of the pristine graphite electrode (a) and EAGE (b) (the insert shows the corresponding image in the high frequency region) in $2 \text{ mol}\cdot\text{dm}^{-3} \text{ H}_2\text{SO}_4+2 \text{ mol}\cdot\text{dm}^{-3} \text{ VOSO}_4$ solution for different polarization potentials

The Nyquist plots of the pristine graphite electrode and EAGE in $2 \text{ mol}\cdot\text{dm}^{-3} \text{ H}_2\text{SO}_4+2 \text{ mol}\cdot\text{dm}^{-3} \text{ VOSO}_4$ solution at different polarization potentials are shown in Fig. 5. The Fig. 5a shows that, the experimental curves have the shape of a semi-circle in the high frequency region, whereas it is a straight line with a slope of unity approximately in the low frequency region. This indicates that the anodic oxidation of V(IV) on the pristine graphite electrode is a mixed kinetic-diffusion controlled process. However, for EAGE, the diameter of semi-circle in the high frequency region is much smaller than that on the pristine graphite electrode, which is shown in the insert of Fig. 5b. These suggest that the reaction rate of the anodic oxidation of V(IV) on EAGE is much higher than that on the pristine graphite electrode, which is in agreement with the results of cyclic voltammograms shown in Fig. 4 and the standard rate constant, k_0 , evaluated from Fig. S1a and Fig. S1b.

Fig. 6 shows the cyclic voltammograms of the pristine graphite

electrode and EAGE in $2 \text{ mol}\cdot\text{dm}^{-3} \text{ H}_2\text{SO}_4 + 2 \text{ mol}\cdot\text{dm}^{-3} \text{ V(III)}$ solution with different scan rates. By comparison with Fig. 6a, It is obvious that both the anodic peak and the cathodic peak current density (i_p) of V(II)/V(III) couple increase significantly on EAGE as shown in Fig. 6b. Furthermore, the peak potential separation (ΔE_p) on the pristine graphite electrode and EAGE decreases from 405 to 138 mV at the scan rate of $20 \text{ mV}\cdot\text{s}^{-1}$, respectively. This means that the V(II)/V(III) couple on EAGA displays much better electrochemical activity and reversibility than that on the pristine graphite electrode.

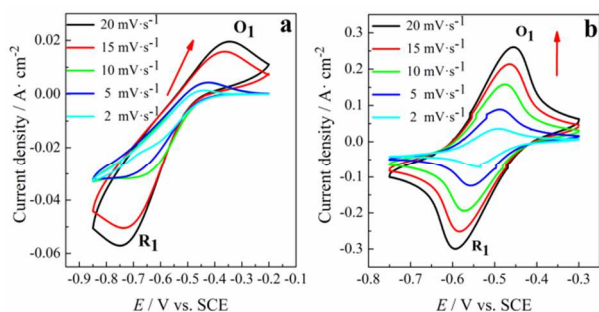


Fig. 6. The cyclic voltammograms of the pristine graphite electrode (a) and EAGE (b) in $2 \text{ mol}\cdot\text{dm}^{-3} \text{ H}_2\text{SO}_4 + 2 \text{ mol}\cdot\text{dm}^{-3} \text{ V(III)}$ solution with different scan rates

According to the typical examples of cyclic voltammograms shown in Fig. 6, the relationship between $\ln i_p$ and $(E_p - E_0)$ for the reduction of V(III) on EAGE can be obtained and shown in the supporting information Fig. S2. Therefore, the rate constant of charge transfer for the cathodic reduction of V(III), k_{θ} , on EAGE is calculated as $1.12 \times 10^{-3} \text{ cm}\cdot\text{s}^{-1}$, which is even larger than that on the anodic oxidation of V(IV) on EAGE. This may be due to the V(II)/V(III) redox reaction more strongly depends on the formation of surface active functional groups of C-OH and COOH than dose the V(IV)/V(V) redox reaction.

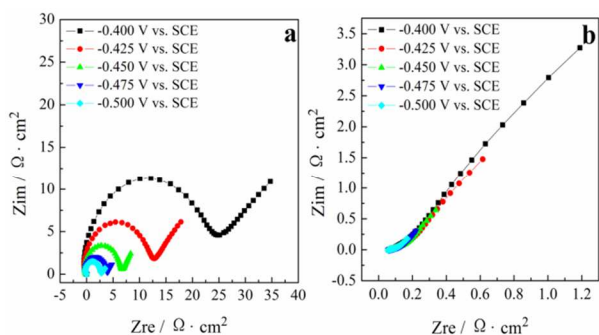


Fig. 7. Nyquist plots of the pristine graphite electrode (a) and EAGE (b) in $2 \text{ mol}\cdot\text{dm}^{-3} \text{ H}_2\text{SO}_4 + 2 \text{ mol}\cdot\text{dm}^{-3} \text{ V(III)}$ solution at different polarization potentials

The Nyquist plots of the pristine graphite electrode and EAGE in $2 \text{ mol}\cdot\text{dm}^{-3} \text{ H}_2\text{SO}_4 + 2 \text{ mol}\cdot\text{dm}^{-3} \text{ V(III)}$ solution at different polarization potentials are shown in Fig. 7. From Fig. 7a, we can conclude that, the cathodic reduction of V(III) on the pristine graphite electrode is a mixed kinetic-diffusion controlled process. However, for EAGE, it is a straight line with a slope of unity approximately in the frequency region from 10^{-2} to 10^5 Hz, which indicates that cathodic reduction of V(III) on EAGE is a completely diffusion controlled process. In other words, the

reaction rate of the cathodic reduction of V(III) on EAGE is much higher than that on the pristine graphite electrode. These results are consistent with the cyclic voltammograms as shown in Fig. 6.

4. Conclusions

The EAGE is obtained by a simple and moderate method of anodic potentiostatic polarization of the graphite electrode in $2 \text{ mol}\cdot\text{dm}^{-3} \text{ H}_2\text{SO}_4$. The electrode processes of V(II)/V(III), V(III)/V(IV), and V(IV)/V(V) couples with better reversibility are firstly and simultaneously obtained on an electrochemical modified graphite electrode.

The electrochemical activity and the reversibility for electrode processes of V(II)/V(III) and V(IV)/V(V) couples are significantly enhanced on EAGE, which is due to the functional groups of C=O and COOH introduced on the surface of EAGE. The rate constant of charge transfer for the anodic oxidation of V(IV) on EAGE is evaluated as $8.17 \times 10^{-4} \text{ cm}\cdot\text{s}^{-1}$, which is about 20 times larger than that on the pristine graphite electrode of $4.09 \times 10^{-5} \text{ cm}\cdot\text{s}^{-1}$. Meanwhile, the rate constant of charge transfer for the cathodic reduction of V(III) on EAGE is calculated as $1.12 \times 10^{-3} \text{ cm}\cdot\text{s}^{-1}$.

60 Acknowledgments

The authors acknowledge the financial support of National Basic Research Program of China (Grant No. 2010CB227203) and the financial support of the Fundamental Research Funds for the Central Universities (Grant No. N100602009).

65 References

- 1 E. Sum, M. Rychcik and M. Skyllas-Kazacos, J. Power Sources, 1985, **16**, 85.
- 2 M. H. Chakrabarti, R. A. W. Dryfe and E. P. L. Roberts, Electrochim. Acta, 2007, **52**, 2189.
- 3 M. Skyllas-Kazacos, M. H. Chakrabarti, S. A. Hajimolana, F. S. Mjalli and M. Saleem, J. Electrochem. Soc, 2011, **158**, R55.
- 4 P. Leung, X. H. Li, C. P. de Leo'n, L. Berlouis, C. T. John Low and F. C. Walsh, RSC Advances, 2012, **2**, 10125.
- 5 S. Zhong, C. Padeste, M. Kazacos and M. Skyllas-Kazacos, J. Power Sources, 1993, **45**, 29.
- 6 D. S. Aaron, Q. Liu, Z. Tang, G. M. Grim, A. B. Papandrew, A. Turhan, T. A. Zawodzinski and M. M. Mench, J. Power Sources, 2012, **206**, 450.
- 7 H. Kaneko, K. Nozaki, Y. Wada, T. Aoki, A. Negishi and M. Kamimoto, Electrochim. Acta, 1991, **36**, 1191.
- 8 H. J. Liu, T. T. Cai, Q. S. Song, L. X. Yang, Q. Xu and C. W. Yan, Int. J. Electrochem. Sci., 2013, **8**, 2515.
- 9 B. Sun and M. Skyllas-Kazacos, Electrochim. Acta, 1991, **36**, 513.
- 10 N. Yabuuchi, B. M. Gallant, S. Chen, B. S. Kim, P. T. Hammond and Y. Shao-Horn, Nature Nanotechnology, 2010, **5**, 531.
- 11 B. Sun and M. Skyllas-kazacos, Electrochim. Acta, 1992, **37**, 2459.
- 12 K. Kim, Y. Kim, J. Kim and M. Park, Mater. Chem. Phys, 2011, **131**, 547.
- 13 L. Yue, W. S. Li, F. Q. Sun, L. Z. Zhao and L. D. Xing, Carbon, 2010, **48**, 3079.
- 14 P. X. Han, H. B. Wang, Z. H. Liu, X. Chen, W. Ma, J. H. Yao, Y. W. Zhu and G. L. Cui, Carbon, 2011, **49**, 693.
- 15 W. Y. Li, J. G. Liu and C. W. Yan, Carbon, 2013, **55**, 313.
- 16 T. Wu, K. L. Huang, S. Q. Liu, S. X. Zhuang, D. Fang, S. Li, D. Lu and A. Q. Su, J. Solid State Chem., 2012, **16**, 579.

- 17 H. J. Liu, Q. Xu, C. W. Yan and Y. L. Qiao, *Electrochim. Acta*, 2011, **56**, 8783.
- 18 Y. Q. Wang, H. Viswanathan, A. A. Audi and P. M. A. Sherwood, *Chem. Mater.*, 2000, **12**, 1100.
- 5 19 E. Desimoni, G. I. Casella, A. Monroe and A. M. Salvi, *Surf. Interface Anal.*, 1990, **15**, 627.
- 20 Y. Shao, J. Wang, R. Kou, M. Engelhard, J. Liu and Y. Wang, *Electrochim. Acta*, 2009, **54**, 3109.
- 21 E. Desimoni, G. I. Casella and A. M. Salvi, *Carbon*, 1992, **30**, 521.
- 10 22 H. Darmstadt, C. Roy and S. Kallaguine, *Carbon*, 1994, **32**, 1399.
- 23 H. Estrade-Szwarckopf, *Carbon*, 2004, **42**, 1713.
- 24 W. Y. Li, J. G. Liu and C. W. Yan, *Carbon*, 2011, **49**, 3463.
- 25 O. V. Cherstiouk, P. A. Simonov, V. B. Fenelonov and E. R. Savinova, *J. Appl. Electrochem.*, 2010, **40**, 1933.
- 15 26 W. H. Wang and X. D. Wang, *Electrochim. Acta*, 2007, **52**, 6755.
- 27 C. A. McDermott, K. R. Kneten and L. McCreery, *J. Electrochem. Soc.*, 1993, **140**, 2593.
- 28 M. T. McDermott, K. Kneten and R. L. McCreery, *J. Phys. Chem.*, 1992, **96**, 3124.
- 20 29 P. H. Chen and R. L. McCreery, *Anal. Chem.*, 1996, **68**, 3958.
- 30 C. E. Banks, T. J. Davies, G. G. Wildgoose and R. G. Compton, *Chem. Commun.*, 2005, **7**, 829.
- 31 A. J. Bard and L. R. Faulkner, *Electrochemical Methods-Fundamentals and Applications*, Wiley-Interscience, New York, 2nd edn, 2001.
- 25 32 B. Sun and M. Skyllas-Kazacos, *Electrochim. Acta*, 1992, **37**, 1253.

Graphical abstract

The electrochemical activity of the graphite electrode and the reversibility for electrode processes of vanadium ions redox couples are significantly enhanced on EAGE, which is due to the functional groups of COOH and C=O introduced on the surface of graphite electrode during electrochemical activation.

